Polymer Journal, Vol. 37, No. 2, pp. 65–73 (2005)

Mutual- and Self-Diffusion Coefficients of a Semiflexible Polymer in Solution

Takayuki KANEMATSU,[1,††] Takahiro SATO,[1,†] Yasuhito IMAI,[2]
Koichi UTE,[2] and Tatsuki KITAYAMA[2]

[1]*Department of Macromolecular Science, Osaka University, 1-1 Machikaneyama-cho, Toyonaka 560-0043, Japan*
[2]*Department of Chemistry, Faculty of Engineering Science, Osaka University, 1-3 Machikaneyama-cho, Toyonaka 560-8531, Japan*

(Received September 1, 2004; Accepted October 27, 2004; Published February 15, 2005)

ABSTRACT: Mutual- and self-diffusion coefficients of a semiflexible polymer, cellulose tris(phenyl carbamate) (CTC), in tetrahydrofuran were measured by dynamic light scattering and pulsed field gradient NMR, respectively, as functions of the polymer concentration and molecular weight. The mutual-diffusion coefficient after elimination of the effects of thermodynamic force and solvent back flow agrees with the self-diffusion coefficient for a low molecular weight CTC fraction with the number of Kuhn's statistical segments $N = 1.8$ up to high concentrations, but they disagree for a higher molecular weight CTC fraction with $N = 4.7$ at the highest concentration investigated. The mutual diffusion coefficients for CTC fractions with N ranging from 1.8 to 10.6 after elimination of the above two effects were also compared with the fuzzy cylinder theory for the self-diffusion coefficient. Disagreements start at lower concentration for larger N, which form in a contrast with good agreements for a more stiff polymer, poly(*n*-hexyl isocyanate), previously studied. [DOI 10.1295/polymj.37.65]

KEY WORDS Mutual-Diffusion Coefficient / Self-Diffusion Coefficient / Dynamic Light Scattering / Pulsed Field Gradient NMR / Semiflexible Polymer / Cellulose Derivative /

There are two kinds of translational diffusion coefficients for binary solution systems: the mutual-diffusion coefficient D_m and the self-diffusion coefficient D_s.[1–3] The conventional concentration gradient method provides the former diffusion coefficient. Dynamic light scattering is a more convenient method to determine D_m, where the concentration gradient is generated by thermal fluctuation. On the other hand, a certain solute molecule is labeled, and the Brownian motion of the labeled molecule (the tracer) is monitored by some method to measure the latter diffusion coefficient D_s. Forced Rayleigh scattering, fluorescence recovery after photobleaching, pulsed field gradient NMR, and so on belong to techniques to measure D_s.[3,4] These two diffusion coefficients are identical at infinite dilution, but they often exhibit opposite concentration dependencies.

The mutual and self diffusions occur under different experimental conditions. While the solution is thermodynamically homogeneous during the measurement of D_s, the concentration gradient is necessary to measure D_m. The concentration gradient provides a thermodynamic force to make a macroscopic flow of the solute at a finite concentration, and the solute flow is accompanied by the solvent back flow to maintain the constant density of the solution. The thermodynamic force and the solvent back flow discriminate D_m from D_s, and the two effects may be eliminated by use of the following equation:[3]

$$\tilde{D} \equiv D_m/[(M/RT)(\partial\Pi/\partial c)(1 - \bar{v}c)] \qquad (1)$$

where M, c, and $\bar{v}$ are the molecular weight, the mass concentration, and the partial specific volume of the solute, respectively, RT is the gas constant multiplied by the absolute temperature, and Π is the osmotic pressure. The effects of the thermodynamic force and the solvent back flow are taken into account by the factors $(M/RT)(\partial\Pi/\partial c)$ and $1 - \bar{v}c$, respectively. This new diffusion coefficient $\tilde{D}$ exhibits a negative concentration dependence, and is comparable with the self-diffusion coefficient D_s.

Kitchen *et al.*[5] and more recently Le Bon *et al.*[6] showed that $\tilde{D}$ agreed well with D_s for aqueous solutions of globular proteins up to considerably high concentrations. Ohshima *et al.*[7] demonstrated that experimental results of $\tilde{D}$ for semidilute solutions of a stiff polymer poly(*n*-hexyl isocyanate) (PHIC) were favorably compared with a theory for D_s. However, Callaghan and Pinder[8] and also Brown *et al.*[9,10] reported that $\tilde{D}$ and D_s were not identical for flexible polymer solutions. Moreover, de Gennes[1] pointed out that the mutual diffusion in entangled polymer solutions might

†To whom correspondence should be addressed (Tel&Fax: +81-6-6850-5461, E-mail: tsato@chem.sci.osaka-u.ac.jp).
††Present Address: Dainippon Ink and Chemicals, Inc., Kansai R & D Center, 1-3 Takasago, Takaishi 592-0001, Japan

Table I. Molecular characteristics of cellulose tris(phenyl carbamate) fractions used[12]

Fraction	$M_w/10^4$	M_w/M_n	DS[a]	N[b]	c^*[c] (g cm^{-3})	D_0 (10^{-7} cm^2 s^{-1})	k_D (cm^3 g^{-1})
F20	3.94	1.06		1.80	0.028		13[d]
F19	4.06	1.08	2.8	1.86	0.027	8.55	13
F17	6.42			2.94	0.016	6.72	23
F16	10.3	1.08		4.72	0.0091	4.50	35
F14	15.0	1.05	3.0	6.87	0.0065	3.85	39
F12	23.2	1.07	3.1	10.6	0.0041	2.89	51

[a]Degree of substitution estimated by elemental analysis. [b]Number of Kuhn's statistical segments calculated from M_w with the molar mass per unit contour length $M_L = 1040\,\mathrm{nm}^{-1}$ and the persistence length $q = 10.5$ nm. [c]Overlap concentration calculated by $c^* = 3M_w/4\pi N_A\langle S^2\rangle^{3/2}$, where N_A is the Avogadro constant, and $\langle S^2\rangle$ is the mean-square radius of gyration determined previously by light scattering (fractions F16, F14, and F12) or calculated by the Benoit–Doty equation[31] with the above q and N (for fractions F20, F19, and F17). [d]Assumed value.

take place without disentanglement, which is necessary in the case of the self diffusion. Nonequilibrium statistical mechanics verifies the non-identity of the two diffusion coefficients,[11] but cannot answer how much the difference is.

The present study was undertaken to elucidate the relation between the mutual- and self-diffusion coefficients in entangled polymer solutions. The previous studies imply that the polymer chain stiffness is a key parameter in that relation. Thus, we chose as a test sample a cellulose derivative, cellulose tris(phenyl carbamate) (CTC), with a chain stiffness intermediate between typical stiff and flexible polymers. This polymer was molecularly well characterized in the previous study.[12] By dynamic light scattering, static light scattering, and pulsed field gradient NMR (PFG-NMR), we have determined D_m, $\partial\Pi/\partial c$, and D_s, respectively, as functions of the concentration and molecular weight of CTC, and compared experimental $\tilde{D}$ and D_s, as well as the fuzzy cylinder theory[13,14] for D_s which was favorably compared with $\tilde{D}$ for PHIC solutions.[7]

EXPERIMENTAL

CTC Fractions

Among CTC fractions used in previous studies,[12,15] six fractions were chosen for diffusion measurements. The preparation and fractionation methods of the fractions were described in a previous paper,[12] and molecular characteristics previously obtained by light scattering and SEC are listed in Table I. The full substitution of CTC fractions was checked previously by elemental analysis.[12] Ratios of the weight- to number-average molecular weight M_w/M_n estimated by SEC are less than 1.1, guaranteeing narrow molecular weight distributions of the fractions used.

Table I also contains the number of Kuhn's statistical segments N of each fraction in tetrahydrofuran (THF), calculated from M_w by using the molar mass per unit contour length $M_L = 1040\,\mathrm{nm}^{-1}$ and the persistence length $q = 10.5$ nm determined previously,[12] as well as the overlap concentration c^*.

Pulsed Field Gradient NMR (PFG-NMR)

NMR measurements were performed for fractions F16 and F20 dissolved in THF-d_8 at 25 °C on a Varian Unity-INOVA 750 spectrometer operating at a proton NMR frequency of 750 MHz using an ^{1}H{^{15}N–^{31}P} 5-mm indirect probe (fraction F20) and an ^{1}H{^{13}C/^{15}N} 5-mm triple resonance probe (fraction F16) with pulsed field gradient coils. Test solutions in precision co-axial tube inserts of 2 mm o.d. (*cf.* Figure 1a) were set in the spectrometer, and the DBPPSTE (Dosy

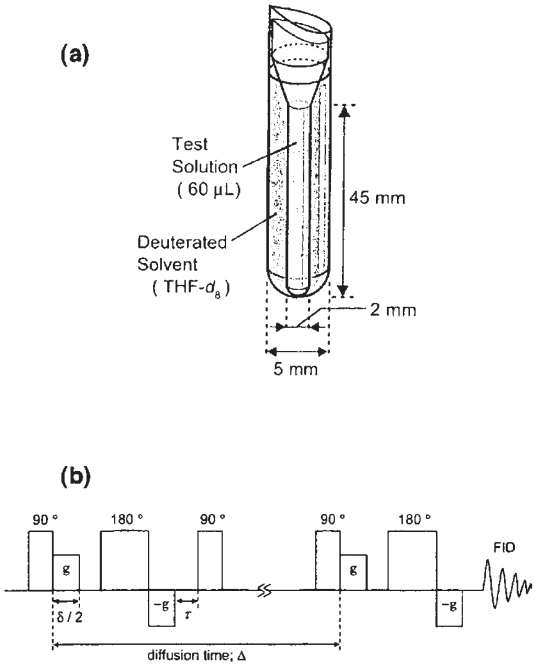

Figure 1. (a) Precision co-axial tube set and (b) the DBPPSTE pulse sequence used for PFG-NMR.

Table II. Experimental conditions in PFG-NMR and results of the self-diffusion coefficient obtained

Fraction	$c/10^{-2}$ g cm^{-3}	Number of transients[a]	g/g cm^{-1}	Δ/s	$D_{s,w}/10^{-7}$ cm^2 s^{-1}			$D_{s,z}/10^{-7}$ cm^2 s^{-1}	
					DECRA	CONTIN[c]	MEM[c]	CONTIN	MEM
F20	7.40	16	14–60	0.80	1.99	2.0 ± 0.5	2.1 ± 0.5	1.85	1.72
	4.70	16	14–60	0.50	3.42	3.4 ± 0.2	3.5 ± 0.6	3.40	2.44
	2.52	64	20–60	0.20	5.20	5.3 ± 1.2	5.2 ± 1.5	4.92	3.82
	0.940	128	20–60	0.20	7.16	7.5 ± 2.1	8.0 ± 2.1	6.67	6.82
	0.381	128	20–60	0.20	8.30	9.0 ± 3.1	8.4 ± 1.8	7.45	7.84
	0.134	128	20–60	0.20	8.81	10.1 ± 4.6	8.7 ± 1.3	7.42	8.39
F16	4.93	256	20–60	2.30	0.75	0.79 ± 0.2	0.75 ± 0.8	0.750	0.749
	2.83	128	20–60	1.00	1.51	1.5 ± 0.4	1.5 ± 0.5	1.45	1.42
	1.03	512	20–60	0.60	2.74	2.8 ± 0.4	2.8 ± 0.3	2.72	2.79
	0.313	128	20–60	0.55	4.03	4.4 ± 1.1	NC[b]	3.97	NC[b]
	0.140	512	20–60	0.50	3.93	5.3 ± 3.1	3.5 ± 0.5	3.31	3.44

[a]Recycle delay, 14 s. [b]Not converged. [c]Values are means $\pm$ estimated standard deviations.

Bipolar Pulsed Pair STimulated Echo) sequence[16] illustrated in Figure 1b was applied, where the width of the pulsed gradient δ and the gradient recover time τ were chosen to be 2 ms and 0.3 ms, respectively. The diffusion time, Δ, ranged from 200 ms to 2.3 s, and 20 echoes were acquired at different values of the gradient amplitude, g, from 14 to 60 or 20 to 60 G/cm; the PFG-NMR parameters chosen for each solution are summarized in Table II.

The variation of integrated peak intensity $I(g)$ with g depends on the self-diffusion coefficient of components responsible for the absorption peak. If the diffusing component is polydisperse, $I(g)$ can be written in the form

$$I(g) = \sum_i G(D_{s,i}) \exp\left[-(\gamma g \delta)^2 \left(\Delta - \frac{1}{3}\delta - \frac{1}{2}\tau\right) D_{s,i}\right] \quad (2)$$

where $D_{s,i}$ is the self-diffusion coefficient of the component i, $G(D_{s,i})$ is the mole fraction of the chemical group belonging to the component i which causes the absorption peak, and the summation is taken over all components responsible for the absorption peak. The inverse Laplace transform (ILT) of $I(g)$ provides the distribution $G(D_{s,i})$. The Direct Exponential Curve Resolution Algorithm (DECRA),[17,18] CONTIN,[19] and Maximum Entropy Method (MEM)[20] were used for the inverse Laplace transform to obtain $G(D_{s,i})$.

In this study, the absorption peak arising from the phenyl ring in CTC was used for the PFG-NMR analysis. Since every glucose residue of CTC has three phenyl groups, $G(D_{s,i})$ in eq 2 is equal to the weight fraction of the CTC component with the self-diffusion coefficient $D_{s,i}$, and the weight-average self-diffusion coefficient $D_{s,w}$ is simply calculated by

$$D_{s,w} = \sum_i D_{s,i} G(D_{s,i}) \quad (3)$$

On the other hand, the z-average self-diffusion coefficient $D_{s,z}$ is estimated by

$$D_{s,z} = \sum_i D_{s,i}^{1-1/\alpha} G(D_{s,i}) \Big/ \sum_i D_{s,i}^{-1/\alpha} G(D_{s,i}) \quad (4)$$

where α is the power-law exponent in the molecular weight dependence of D_s.

Light Scattering

Mutual diffusion coefficients were determined as functions of the polymer concentration c by dynamic light scattering for THF solutions of five CTC fractions (F19, F17, F16, F14, and F12) at 25 °C with an ALV/DLS/SLS-5000 light scattering system. Osmotic compressibilities for THF solutions of the five CTC fractions were also measured as functions of c at 25 °C with a Fica 50 light scattering photometer or the above ALV system. Vertically polarized light with the wavelength of 532 nm (ALV) or of 546 nm (Fica) was used as the incident light, and the scattered light was measured with no analyzer. Test solutions were prepared in the same procedure as that applied in the previous work.[12]

Dynamic light scattering provides us the intensity autocorrelation function $g^{(2)}(t)$, and the first cumulant Γ defined by

$$\Gamma \equiv \frac{1}{2} \lim_{t \to 0} \mathrm{d} \ln[g^{(2)}(t) - 1]/\mathrm{d}t \quad (5)$$

The z-average mutual diffusion coefficient $D_{m,z}$ was determined from Γ by

$$D_{m,z} = \lim_{k \to 0} \Gamma/k^2 \quad (6)$$

where k is the magnitude of the scattering vector. On the other hand, the procedure to obtain the reciprocal of osmotic compressibility $\partial\Pi/\partial c$ from static light scattering was explained in the previous paper.[12]

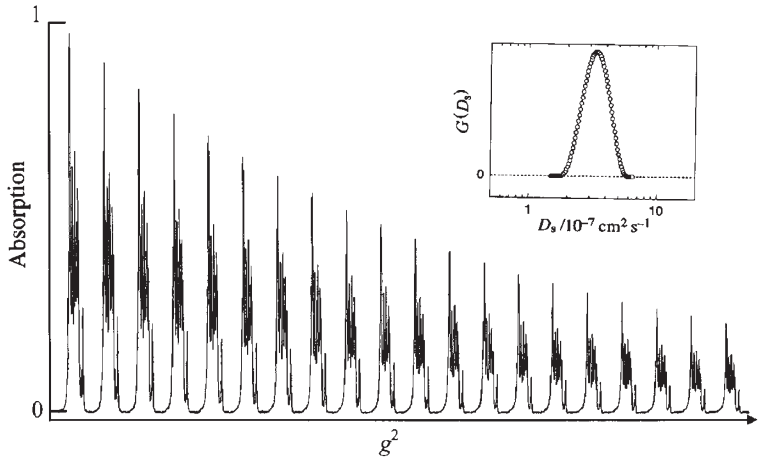

Figure 2. Variation of the absorption peaks arising from phenyl groups of CTC with the square g^2 of the magnetic field gradient in a THF-d_8 solution of fraction F20 with $c = 4.70 \times 10^{-2}$ g/cm^3 at 25 °C. The vertical axis is normalized by the highest peak height at $g^2 = 0$.

RESULTS

Figure 2 shows the result of PFG-NMR obtained for a THF-d_8 solution of fraction F20 with the polymer mass concentration $c = 0.0470$ g/cm^3. The absorption peaks arising from the phenyl group in CTC around 7 ppm diminish with increasing the square g^2 of the magnetic field gradient. The decay of the integrated peak intensity $I(g)$ for the phenyl group were analyzed by DECRA, CONTIN, and MEM to obtain the distribution $G(D_s)$ of the self-diffusion coefficient D_s. The result of the CONTIN analysis for $I(g)$ in Figure 2 is shown in the insert of the same figure. The distribution $G(D_s)$ is narrow, corresponding to the narrow molecular weight distribution of the CTC fraction (*cf.* Table I).

Table II summarizes weight-average self-diffusion coefficients $D_{s,w}$ estimated from $G(D_s)$ using eq 3 for fractions F20 and F16. Standard deviations in $D_{s,w}$ were estimated from errors in the fittings by CONTIN and MEM. The different ILT analyses provide almost identical $D_{s,w}$ except at the lowest c for both fractions, indicating good performance of the ILT algorisms. The disagreements of $D_{s,w}$ estimated from the different ILT, as well as considerably large standard deviations, at the lowest c come from the low signal to noise ratio of $I(g)$. Table II also lists results of the z-average self-diffusion coefficient $D_{s,z}$ calculated by eq 4, where the exponent α at each c was estimated from the data of $D_{s,w}$ and M_w for the two fractions F20 and F16; for the lowest c, α was chosen to be 0.62.[12] The difference between $D_{s,w}$ and $D_{s,z}$ is small except at the lowest c. Figure 3 shows the concentration dependence of $D_{s,w}$ and $D_{s,z}$ obtained by CONTIN. For both fractions, the diffusion coefficients look to start decreasing sharply beyond c^* (*cf.* Table I).

Figure 4 shows the plot of $\ln[g^{(2)}(t) - 1]$ against k^2t for a THF solution of fraction F16 with $c = 0.0666$ g/cm^3 measured at different scattering angles θ. The data points follow straight lines within the k^2t range displayed, and Γ/k^2 estimated from the slopes of the lines indicated are independent of θ or k for this fraction. Among five CTC fractions investigated by dynamic light scattering, only the highest molecular weight fraction F12 exhibits a weak negative k^2 dependence of Γ/k^2 at high c, as shown in Figure 5. Similar negative k^2 dependencies of Γ/k^2 at high c was observed previously for poly(γ-benzyl L-glutamate)[21] and poly(*n*-hexyl isocyanate) solutions,[7] and qualitatively explained by Doi *et al.*[22] The mutual diffusion coefficient $D_{m,z}$ was estimated by the extrapolation of Γ/k^2 to zero k. This extrapolation assures us that $D_{m,z}$ is the diffusion coefficient for the concentration fluctuation with the wavelength much larger than the individual polymer chain size and that the internal (or intramolecular) motion of polymer chain segments has nothing to do with $D_{m,z}$. The results of

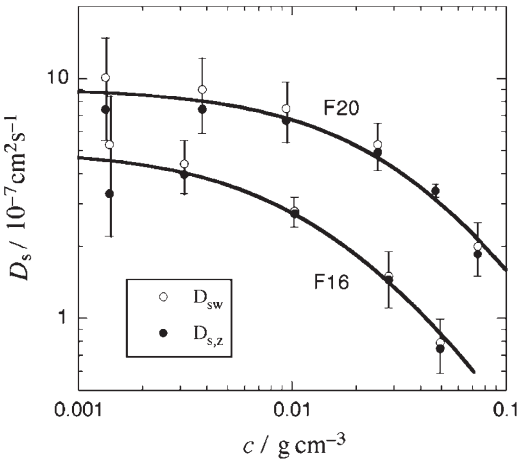

Figure 3. Concentration dependence of D_s for THF-d_8 solutions of two CTC fractions at 25 °C. Solid curves are eye guide.

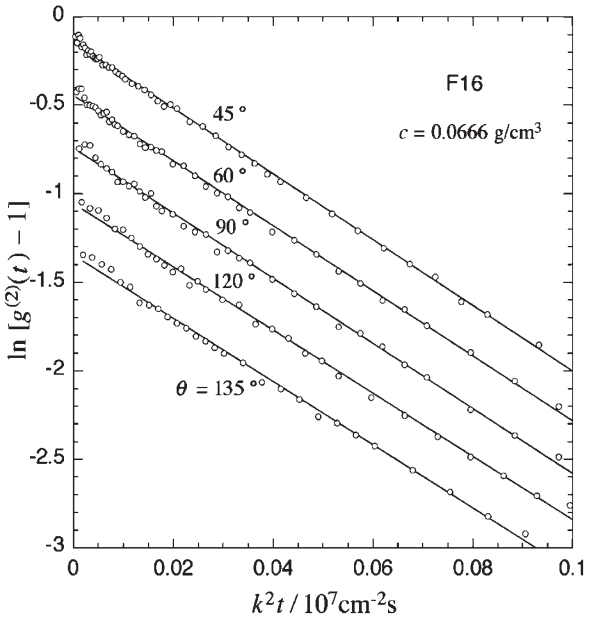

Figure 4. Plots of $\ln[g^{(2)}(t) - 1]$ *vs.* k^2t for a THF solution of fraction F16 with $c = 6.66 \times 10^{-2}$ g/cm^3 at 25 °C. Data points except at $\theta = 45°$ are shifted downwards by different amounts for the viewing clarity.

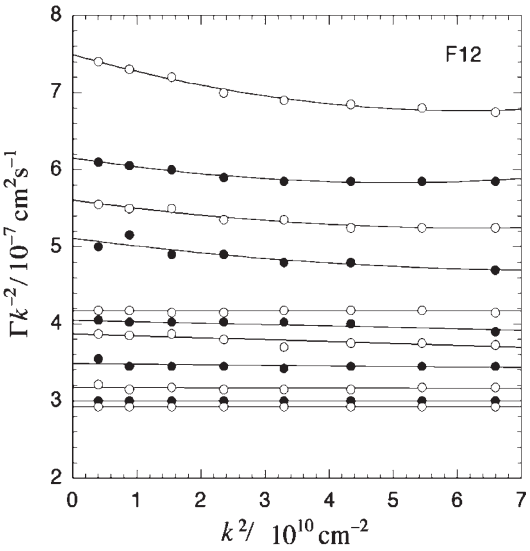

Figure 5. Dependence of Γ/k^2 on k^2 for THF solutions of fraction F12; $c/10^{-2}$ g cm^{-3} = 3.87, 2.63, 2.08, 1.60, 0.968, 0.850, 0.768, 0.668, 0.606, 0.394, 0.291, 0.188, 0.127, 0.112, 0.0942, 0.0668, 0.0464, 0.0239 from the top to bottom.

$D_{m,z}$ obtained for THF solutions of the five CTC fractions are plotted against c in Figure 6. For all the fractions, $D_{m,z}$ monotonically increases with c. For the three high molecular weight fractions, $D_{m,z}$ becomes almost independent of the molecular weight, at high c.

Figure 7 shows the concentration dependence of $(RT)^{-1}\partial\Pi/\partial c$ for the same five CTC fractions obtained by static light scattering. This quantity also monotonically increases with c. Figure 8 presents the quantity $\tilde{D} \equiv D_{m,z}[(M/RT)(\partial\Pi/\partial c)(1 - \bar{\nu}c)]^{-1}$ calcu-

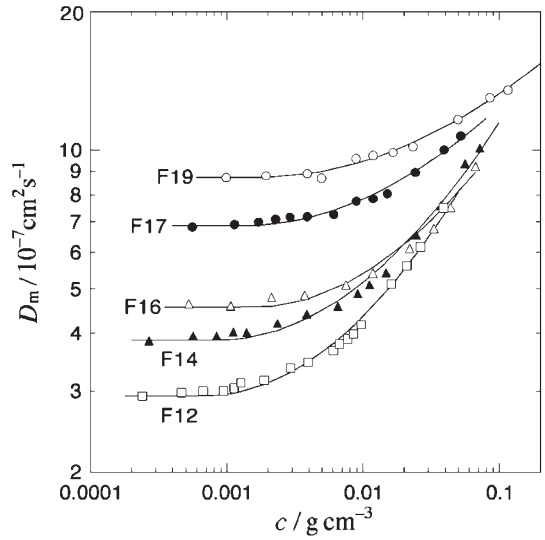

Figure 6. Concentration dependence of D_m for THF solutions of five CTC fractions at 25 °C. Solid curves are eye guide.

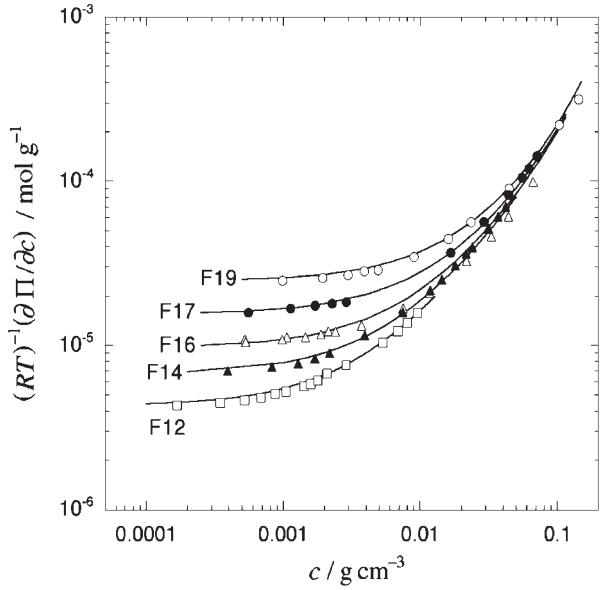

Figure 7. Concentration dependence of $(RT)^{-1}\partial\Pi/\partial c$ for THF solutions of five CTC fractions at 25 °C. Data for fractions F19, F17, and F14 are taken from ref 12, and solid curves are drawn by the scaled particle theory for the wormlike chain considering the soft dispersion interaction (*cf.* ref 12).

lated from the results shown in Figures 6 and 7. We have used 0.716 cm^3/g as the partial specific volume $\bar{\nu}$.[12] Owing to stronger c dependence of $\partial\Pi/\partial c$ than that of $D_{m,z}$, $\tilde{D}$ monotonically decreases with c for all five fractions.

Self-diffusion coefficients $D_{s,z}$ obtained by PFG-NMR for fractions F20 and F16, presented in Figure 3, are plotted also in Figure 8 by filled circles and filled diamonds, respectively. On one hand, $\tilde{D}$ for fraction F19 agrees with $D_{s,z}$ for fraction F20 (with almost the same molecular weight) over the entire c range investigated, which demonstrates that the mobility of in-

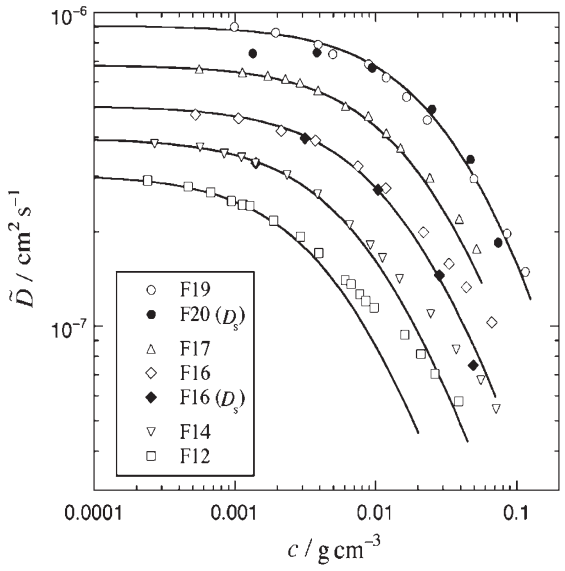

Figure 8. Comparison between D_s obtained by PFG-NMR and $\tilde{D}$ obtained by dynamic and static light scattering (*cf.* eq 1) for five CTC fractions in THF (or THF-d_8) at 25 °C. Solid curves indicate theoretical values of D_s calculated by the fuzzy cylinder theory (eqs 7–10) with $k'_\perp/k'_\parallel = 1.7$.

dividual chains of this CTC fraction in solution is indistinguishable in mutual and self diffusion processes. This is consistent with conclusions of Kitchen *et al.*[5] and Le Bon *et al.*[6] for globular proteins and also of Ohshima *et al.*[7] for a stiff polymer poly(*n*-hexyl isocyanate), in solution over wide concentration ranges. On the other hand, a definite disagreement between $\tilde{D}$ and $D_{s,z}$ is seen for the higher molecular weight fraction F16 at the highest c investigated, although the two diffusion coefficients agree well in an intermediate c range. Therefore, eq 1 cannot convert D_m to D_s for CTC solutions with relatively large N ($\gtrsim 5$) at high concentrations ($c/c^* \gtrsim 3$), indicating that the mutual and self diffusions occur in different modes of polymer dynamics in such solutions.

Invalidity of eq 1 was reported for a flexible polymer polystyrene in semidilute solutions by Callaghan and Pinder.[8] The concentration dependence of their D_s was stronger than that of $\tilde{D}$ obtained by Roots *et al.*[23] for the same polymer, in accordance with our results for fraction F16. On the other hand, Brown *et al.*[9,10] reported the disagreement between $\tilde{D}$ and D_s for aqueous solutions of flexible polymers, poly(ethylene oxide) and dextran, below c^*. Our results show agreements between $\tilde{D}$ and D_s at least below c^*, forming a contrast with Brown *et al.*'s.

DISCUSSION

Fuzzy Cylinder Theory[7,13,14,24]

In a previous paper,[15] the zero-shear viscosity of THF solutions of CTC were demonstrated to be favorably compared with the prediction of the fuzzy cylinder theory. Here we compare the diffusion coefficient data obtained in this study with the same theory. The effective length L_e and diameter d_e of the fuzzy cylinder are defined by $L_e = \langle R^2 \rangle^{1/2}$ and $d_e = (\langle H^2 \rangle + d^2)^{1/2}$, where d is the polymer real diameter, and $\langle R^2 \rangle$ and $\langle H^2 \rangle$ are the mean-square end-to-end distance and mean square distance between the chain midpoint and the end-to-end axis, respectively, both of which can be calculated with the persistence length q and the Kuhn segment number N of the polymer chain. As shown previously,[12] the intramolecular excluded-volume effect is negligible within the molecular weight range of our CTC fractions used in this study, so that we do not consider this effect.

The self-diffusion coefficient D_s may be written as[7,14]

$$D_s = \frac{1}{3}(D_\parallel + 2D_\perp) \tag{7}$$

where $D_\parallel$ and $D_\perp$ are the longitudinal and transverse diffusion coefficients along and perpendicular to the polymer end-to-end axis, respectively. Using the fuzzy cylinder model, we can formulate $D_\parallel$ and $D_\perp$ for stiff or semiflexible polymers in solution ranging from dilute through concentrated (isotropic) regimes.[14] The jamming effect on $D_\parallel$ can be treated on the basis of the hole theory, which gives the following equation[13,14]

$$D_\parallel = \hat{D}_{\parallel 0} \exp(-V^*_{ex} c'), \tag{8}$$

where $\hat{D}_{\parallel 0}$ is $D_\parallel$ without the jamming effect, V^*_{ex} is the excluded volume between the critical hole and a hindering chain, and c' is the polymer number concentration. The critical hole is assumed to be similar in shape to the fuzzy cylinder, and V^*_{ex} is calculated by use of the similarity ratio λ^* of the critical hole to the fuzzy cylinder.

The entanglement effect on $D_\perp$ is treated by a mean-field Green function method,[25,26] The final expression for $D_\perp$ read[14,24]

$$D_\perp = \hat{D}_{\perp 0}\left[1 + \beta_\perp^{-1/2} L_e{}^3 c' \left(1 + C\frac{d_e}{L_e}\right) \times \left(1 + \frac{C}{3}\frac{d_e}{L_e}\right)\left(\frac{2\hat{D}_{\perp 0}}{D_\parallel}\right)^{1/2}\right]^{-2} \tag{9}$$

where $\hat{D}_{\perp 0}$ is the transverse diffusion coefficient at switching off the entanglement effects and $\beta_\perp$ is a constant ($= 560$[27]). The coefficient C is a function of N with two adjustable parameters N^* and Δ.

The diffusion coefficients $\hat{D}_{\parallel 0}$ and $\hat{D}_{\perp 0}$ depend on c through the intermolecular hydrodynamic interaction (HI). If c is not so high, they are written as[24]

$$\hat{D}_{\parallel 0} = D_{\parallel 0}(1 - k'_{\parallel}[\eta]c + \cdots),$$
$$\hat{D}_{\perp 0} = D_{\perp 0}(1 - k'_{\perp}[\eta]c + \cdots) \qquad (10)$$

with two hydrodynamic coefficients $k'_{\parallel}$ and $k'_{\perp}$, where $[\eta]$ is the intrinsic viscosity, and $D_{\parallel 0}$ and $D_{\perp 0}$ are the longitudinal and transverse diffusion coefficients at infinite dilution.

Inserting eqs 8 and 9 with eq 10 into eq 7 and expanding this equation in terms of the power series of c, we have

$$D_s = D_0[1 - (k'_{s,HI} + k'_{s,EI})[\eta]c + \cdots] \qquad (11)$$

with the diffusion coefficient D_0 at infinite dilution, and the coefficients $k'_{s,HI}$ and $k'_{s,EI}$ defined by

$$k'_{s,HI} \equiv \frac{k'_{\parallel} + (2D_{\perp 0}/D_{\parallel 0})k'_{\perp}}{1 + 2D_{\perp 0}/D_{\parallel 0}} \qquad (12)$$

and

$$k'_{s,EI} \equiv \frac{(N_A/[\eta]M)\left[V^*_{ex} + 2\beta_{\perp}^{-1/2}L_e{}^3(1 + Cd_e/L_e)\left(1 + \frac{1}{3}Cd_e/L_e\right)(2D_{\perp 0}/D_{\parallel 0})^{3/2}\right]}{1 + 2D_{\perp 0}/D_{\parallel 0}} \qquad (13)$$

where N_A is the Avogadro constant and M is the polymer molecular weight.

Equation 11 for D_s corresponds to the Huggins equation which writes the reduced viscosity as $\eta_{sp}/c = [\eta]\{1 + (k'_{HI} + k'_{EI})[\eta]c + \cdots\}$.[24] Here, k'_{HI} and k'_{EI} are the intermolecular HI term and the entanglement term of the Huggins coefficient, respectively. The coefficients $k'_{s,HI}$ and $k'_{s,EI}$ in eq 11 are the corresponding coefficients of the intermolecular HI and entanglement for D_s, respectively. On the other hand, the mutual diffusion coefficient D_m of dilute solutions is written as $D_m = D_0(1 + k_D c + \cdots)$. Since we may identify $\tilde{D}$ with D_s at least in the dilute regime as shown in Figure 8, we have the following relation of the coefficient k_D to $k'_{s,HI}$ and $k'_{s,EI}$ from eqs 1 and 11:

$$k_D = 2A_2M - (k'_{s,HI} + k'_{s,EI})[\eta] - \bar{\nu} \qquad (14)$$

where A_2 is the second virial coefficient.

Comparison with Experiment

Most of parameters appearing in the above equations have already determined previously;[12,15] $q = 10.5\,\text{nm}$, $d = 2.2\,\text{nm}$, $\lambda^* = 0.04$, and $N^* = \Delta = 4$. Only unknown parameters are $k'_{\parallel}$ and $k'_{\perp}$. These parameters are related to the HI parameter $k'_{s,HI}$ by eq 12, and $k'_{s,HI}$ can be calculated from experimental quantity k_D by eqs 13 and 14. Table I lists results of k_D estimated from the initial slope of the plot of $D_{m,z}$ *vs.* c (*cf.* Figure 6), and Figure 9 compares $k'_{s,HI}$ calculated from these k_D and the corresponding coefficient $k'_{s,EI}$ arising from the entanglement effect calculated by eq 13 with the known molecular parameters. The former $k'_{s,HI}$ exceeds the latter $k'_{s,EI}$ at large N, but both are comparable at smaller N. Figure 9 also contains the Huggins coefficients k'_{HI} and k'_{EI} for the solution viscosity of the same fractions by the method explained previously.[15] Both effects of the intermolecular HI and entanglement on the first-order concentration dependence of the self-diffusion coefficient are stronger than those of the solution viscosity. It is also noted that the importance of both effects at large N is opposite for diffusion and viscosity.

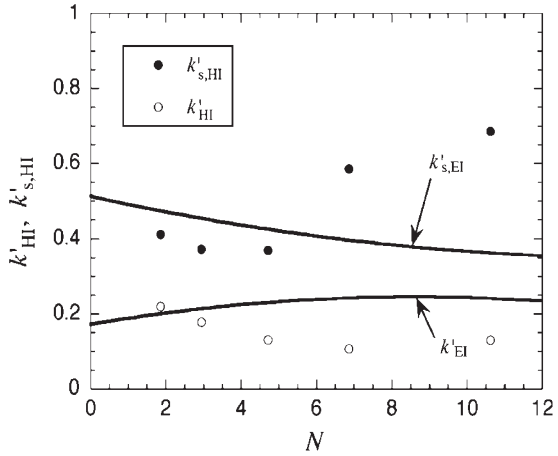

Figure 9. Hydrodynamic coefficients for the first-order concentration dependence of the self-diffusion coefficient and of the solution viscosity. Solid curves indicate $k'_{s,EI}$ and k'_{EI} calculated by eq 13 in the present paper and eq 10 in ref 23, respectively, filled circles show $k'_{s,HI}$ estimated from experimental k_D, A_2, $\bar{\nu}$, and theoretical $k'_{s,EI}$ with eq 13, unfilled circles indicate k'_{HI} estimated from experimental k' and theoretical k'_{EI} with eq 10 in ref 24.

Equation 12 however cannot determine $k'_{\parallel}$ and $k'_{\perp}$ from $k'_{s,HI}$ uniquely. Then we have searched values of $k'_{\parallel}$ and $k'_{\perp}$ leading to best fits of eqs 7–10 to experimental results of $D_{s,z}$ for fractions F20 and F16 under the condition of eq 12. Solid curves in Figure 8 indicate theoretical values of D_s with the ratio $k'_{\perp}/k'_{\parallel}$ fixed to be 1.7. For both fractions F20 and F16, the theoretical curves satisfactorily agree with experimental data of $D_{s,z}$ within the concentration ranges investigated. This demonstrates that the fuzzy cylinder theory can explain both self-diffusivity and solution viscosity for CTC consistently.[28]

On the other hand, the theoretical curves agree with experimental data of $\tilde{D}$ only in restricted c ranges, except for the lowest molecular weight fraction F19. The

deviations start at lower c for fractions with larger N. For the highest molecular weight fraction F12 with $N = 10.6$, the deviation is observed at $c \gtrsim c^*$. The disagreements between the theory and experiment for $\tilde{D}$ is a contrast to good agreements in the zero-shear viscosity η_0 over wider c and N ranges between the fuzzy cylinder theory and experiment demonstrated in the previous paper.[15] For fraction F12, the agreement in η_0 persists far beyond c^*. The disagreement in η_0 was reported at $N \gtrsim 20$,[7,24,29] which was ascribed to the reptation motion of the polymer chain in the mesh formed by surrounding chains which is not considered by the fuzzy cylinder theory. However, the disagreement in the translational diffusion may not come from the reptation motion, because N of our CTC fractions are less than 20.

CONCLUDING REMARKS

The fuzzy cylinder theory deals with the independent translational (or rotational) motion of a certain polymer chain in a homogeneous polymer solution, and is suitable to the argument of the self-diffusion (or tracer-diffusion) coefficient D_s measured by PFG-NMR. On the other hand, the mutual diffusion coefficient D_m obtained by dynamic light scattering is related to a polymer flow in a solution induced by the concentration gradient, and may not necessarily reflect the independent motion of individual polymer chains in the semidilute regime. As mentioned by de Gennes,[1] in a system of overlapping flexible polymer chains, neighboring chains may move together like a sponge without the disentanglement, and this cooperative motion may determine D_m which he called the cooperative diffusion coefficient. The fuzzy cylinder theory does not deal with such a cooperative motion of polymer chains.

However, $\tilde{D}$ for the stiff polymer PHIC with $q = 21\,\text{nm}$ was favorably compared with the fuzzy cylinder theory in a previous study.[7,30] For the highest molecular weight PHIC sample with $N = 26$, the agreement is maintained up to $c/c^* \approx 12$. This indicates that the competition between the independent and cooperative translational motions of the polymer chain in the semidilute regime is not governed only by the parameters N and c/c^*, when one compares polymer solution systems with different q. The competition of the two modes is also a theoretically interesting and naive problem in polymer dynamics.

Acknowledgment. This work was supported by a Grant-in-Aid for Scientific Research from the Ministry of Education, Culture, Sports, Science and Technology of Japan. The authors are grateful to Venture Buisiness Laboratory, Osaka University, Japan for assistance in performing the PFG-NMR experiments on a 750 MHz NMR spectrometer.

REFERENCES

1. P.-G. de Gennes, "Scaling Concepts in Polymer Physics," Cornell University Press, Ithaca, N.Y., 1979.
2. M. Doi and S. F. Edwards, "The Theory of Polymer Dynamics," Clarendon Press, Oxford, U.K., 1986.
3. H. Fujita, "Polymer Solutions," Elsevier, Amsterdam, 1990.
4. M. Tirrell, *Rubber Chem. Technol.*, **57**, 52 (1984).
5. R. G. Kitchen, B. N. Preston, and J. D. Wells, *J. Polym. Sci., Polym. Symp.*, **55**, 39 (1976).
6. C. Le Bon, T. Nicolai, M. E. Kuil, and J. G. Hollander, *J. Phys. Chem. B*, **103**, 10294 (1999).
7. A. Ohshima, A. Yamagata, T. Sato, and A. Teramoto, *Macromolecules*, **32**, 8645 (1999).
8. P. T. Callaghan and D. N. Pinder, *Macromolecules*, **14**, 1334 (1981).
9. W. Brown, P. Stilbs, and R. M. Johnsen, *J. Polym. Sci., Polym. Phys. Ed.*, **20**, 1771 (1982).
10. W. Brown, P. Stilbs, and R. M. Johnsen, *J. Polym. Sci., Polym. Phys. Ed.*, **21**, 1029 (1983).
11. J. A. Marqusee and J. M. Deutch, *J. Chem. Phys.*, **73**, 5396 (1980).
12. F. Kasabo, T. Kanematsu, T. Nakagawa, T. Sato, and A. Teramoto, *Macromolecules*, **33**, 2748 (2000).
13. T. Sato, Y. Takada, and A. Teramoto, *Macromolecules*, **24**, 6220 (1991).
14. T. Sato and A. Teramoto, *Adv. Polym. Sci.*, **126**, 85 (1996).
15. T. Sato, M. Hamada, and A. Teramoto, *Macromolecules*, **36**, 6840 (2003).
16. D. Wu, A. Chen, and C. S. Johnson Jr., *J. Magn. Reson., Ser. A*, **115**, 260 (1995).
17. B. Antalek and W. Windig, *J. Am. Chem. Soc.*, **118**, 10331 (1996).
18. W. Windig and B. Antalek, *Chemom. Intell. Lab. Syst.*, **37**, 241 (1997).
19. S. W. Provencher, *Comput. Phys. Commun.*, **27**, 213 (1982).
20. M. A. Delsuc and T. M. Malliavin, *Anal. Chem.*, **70**, 2146 (1998).
21. P. S. Russo, F. E. Karasz, and K. H. Langley, *J. Chem. Phys.*, **80**, 5312 (1984).
22. M. Doi, T. Shimada, and K. Okano, *J. Chem. Phys.*, **88**, 4070 (1988).
23. J. Roots, B. Nystrom, L. O. Sundelof, and B. Posch, *Polymer*, **20**, 337 (1979).
24. T. Sato, A. Ohshima, and A. Teramoto, *Macromolecules*, **31**, 3094 (1998).
25. S. F. Edwards and K. E. Evans, *J. Chem. Soc., Faraday Trans. 2*, **78**, 113 (1982).
26. I. Teraoka and R. Hayakawa, *J. Chem. Phys.*, **89**, 6989 (1988).
27. I. Teraoka, Ph. D. Thesis, University of Tokyo, 1988.
28. The previous paper indicated that a c^2 term in the intermolecular HI is important in the zero-shear viscosity of THF solutions of fraction F19 with almost the same N as that of fraction F20 (*cf.* Table I) in a high c region. However, as shown in Figure 5 in ref 24, the c^2 term is still minor

at $c \lesssim 0.1\,\mathrm{g/cm^3}$, which is consistent with the use of eq 11 for D_s.

29. A. Ohshima, H. Kudo, T. Sato, and A. Teramoto, *Macromolecules*, **28**, 6095 (1995).
30. In ref 7, both $k'_{\parallel}$ and $k'_{\perp}$ were assumed to be equal with k'_{HI} estimated from the Huggins coefficient. The use of $k'_{\parallel}$ and $k'_{\perp}$ estimated by the same method as in this study provides better agreements between the theory and experiment of $\tilde{\boldsymbol{D}}$ for PHIC solutions.
31. H. Benoit and P. M. Doty, *J. Phys. Chem.*, **57**, 958 (1953).